SF2A 2018
P. Di Matteo, F. Billebaud, F. Herpin, N. Lagarde, J.-B. Marquette, A. Robin, O. Venot (eds)

CLUSTERING ANALYSIS WITH THE SDSS-IV DR14 QUASAR SAMPLE: COSMIC DISTANCES AND GROWTH RATE OF STRUCTURES AT $Z_{\rm EFF} = 1.52$

P. Zarrouk[1] and E. Burtin[*2]

Abstract. The ΛCDM model of cosmology assumes the existence of an exotic component, called dark energy, to explain the late-time acceleration of the expansion of the universe at redshift $z < 0.7$. Alternative scenarios to this cosmological constant suggest to modify the theory of gravitation based on general relativity at cosmological scales. Since fall 2014, the SDSS-IV eBOSS multi-object spectrograph has undertaken a survey of quasars in the almost unexplored redshift range $0.8 \leq z \leq 2.2$ with the key science goal to complement the constraints on dark energy and extend the test of general relativity at higher redshifts by using quasars as direct tracers of the matter field. In this proceeding, I review the clustering measurements of the DR14 quasar sample, which corresponds to two-year data taking of eBOSS, to constrain the cosmic distances, i.e. the angular diameter distance D_A and the expansion rate H, and the growth rate of structure $f\sigma_8$ at an effective redshift $z_{\rm eff} = 1.52$. We also presented the first detection of BAO in a quasar sample Ata et al. (2017) which allows us to constrain the spherically-averaged distance $D_v(z_{\rm eff})$ to 3.8%. In this proceeding, I focus on the anisotropic clustering in configuration space Zarrouk et al. (2018).First, we build large-scale structure catalogues that account for the angular and radial incompleteness of the survey. Then to obtain robust results, we investigate several potential systematics, in particular modeling and observational systematics are studied using dedicated mock catalogs which are fictional realizations of the data sample. These mocks are created with known cosmological parameters such that they are used as a benchmark to test the analysis pipeline. The results on the evolution of distances are consistent with the predictions for ΛCDM with *Planck* parameters assuming a cosmological constant. The measurement of the growth of structure is consistent with general relativity and hence extends its validity to higher redshift. This study is a first use of eBOSS quasars as tracers of the matter field and will be included in the analysis of the final eBOSS sample at the end of 2019 with an expected improvement on the statistical precision of a factor 2. Together with BOSS, eBOSS will pave the way for future programs such as the ground-based Dark Energy Spectroscopic Instrument (DESI) and the space-based mission *Euclid*. Both programs will extensively probe the intermediate redshift range $1 < z < 2$ with millions of spectra, improving the cosmological constraints by an order of magnitude with respect to current measurements.

Keywords: large-scale structures, eBOSS survey, quasars, BAO, RSD

1 Introduction

Spectroscopic surveys are a powerful tool to measure cosmic distances using the position of the Baryon Acoustic Oscillations (BAO) peak in the large-scale structure distribution. The BAO feature in the matter clustering correspond to the imprint left by sound waves from the baryon-photon plasma in the early universe. In this plasma, the high photon-baryon pressure resulted in sound waves propagating at the sound speed $c_s \simeq c/\sqrt{3}$ until the baryons are released from the photons at the drag epoch. The imprint on the matter clustering corresponds to a characteristic scale with wiggles in the power spectrum at $k \sim 0.07, 0.13, 0.19\,h.\mathrm{Mpc}^{-1}$ and to a local enhancement in the two-point correlation function at s $\sim 100\,h^{-1}$.Mpc in comoving units. This signature has been found in luminous red galaxy samples (e.g. SDSS LRG Eisenstein et al. (2005)) and BAO has become

[*]on behalf of the eBOSS Galaxy Quasar Clustering working group

[1] IRFU, CEA, Université Paris-Saclay, F-91191 Gif-sur-Yvette, France; E-mail: pauline.zarrouk@cea.fr. This work received financial support from the P2IO LabEx (reference ANR-10-LABX-0038)

[2] IRFU, CEA, Université Paris-Saclay, F-91191 Gif-sur-Yvette, France

a standard ruler to constrain the evolution of distances and probe the nature of dark energy. Instead of focusing on the BAO peak (BAO-only analysis), full-shape analyses allow us to measure both the expansion history of the universe and the growth of structure, provided thaht the modeling of the two-point anisotropic clustering has been carefully tested as it takes into account non-linearities. Anisotropies arise in the clustering because the observed galaxy redshifts from which distances are measured contain the line-of-sight component of galaxy peculiar velocities driven by the clustering of matter. Such anisotropies are called Redshift Space Distortions (RSD) and encode information on the linear growth rate of structure f. Measuring the evolution of f with redshift has become an important test for the ΛCDM+GR concordance model and it is a key observable for constraining dark energy or modified gravity models (Guzzo et al. 2008).

So far, anisotropic clustering analyses dealt with galaxies as tracers of the matter field (e.g. DR12 BOSS LRG Alam et al. (2017)) to probe the low redshift range ($z < 1$). BOSS and eBOSS also explore the high-redshift range $z > 2.1$ using the Lyman-α forests in quasar spectra as indirect tracers of the neutral hydrogen in the intergalactic medium (IGM). In constrast, eBOSS opens up the $z < 2.2$ redshift range to directly use quasars themselves as cosmological tracers of the matter field.

We measured and analyzed the clustering of the SDSS-IV eBOSS DR14 quasar sample in the redshift range $0.8 \leq z \leq 2.2$ which has been barely unexplored to date by spectroscopic surveys. The current sample corresponds to two-year data taking and includes 148,659 quasars spanning 2112.9 deg^2, which represents almost half of the final footprint that will be completed by the end of February 2019. Using the information from the monopole of both the correlation function and the power spectrum, we perform a BAO-only analysis and present the first detection of the BAO peak in a quasar sample (Ata et al. 2017) which allows us to constrain the spherically-averaged distance $D_v(z_{\rm eff})$ to 3.8%.

We also analyzed the anisotropic clustering of the eBOSS DR14 sample. In this proceeding, I will focus on the study at the effective redshift of the survey $z_{\rm eff} = 1.52$ in configuration space (Zarrouk et al. 2018) using Legendre multipoles with $\ell = 0, 2, 4$ of the correlation function on the s-range from 16 h^{-1}Mpc to 138 h^{-1}Mpc, where μ is the cosine of the angle between the line of sight (LOS) and the orientation vector of the pair of tracers under consideration. I refer the reader to Zarrouk et al. (2018) for detailed references.

2 The SDSS-IV DR14 quasar sample

The footprint of spectroscopically-observed objects is shown in Figure 1. Objects are color-codded by the completeness which encodes information about the survey selection function. This survey selection function can be divided into an angular and radial components. The angular selection function consists in defining a survey mask that corrects for selection effects due to the observational strategy and which will therefore reduce the effective footprint used for clustering analysis. The radial selection function requires to understand the spectroscopic procedure and redshift measurements to ensure that the observed redshift distribution is truly representative of the sample we are analyzing. The eBOSS quasar sample represents a sparse sample with a maximum density of $2 \times 10^{-5} h^3 \mathrm{Mpc}^{-3}$ and an effective redshift of $z_{\rm eff} = 1.52$. While the BOSS galaxy sample can be considered as cosmic-variance limited, the eBOSS quasar sample is in the shot-noise dominated regime with $nP << 1$, where n is the observed quasar density and P is the amplitude of the power spectrum at the scale of interest.

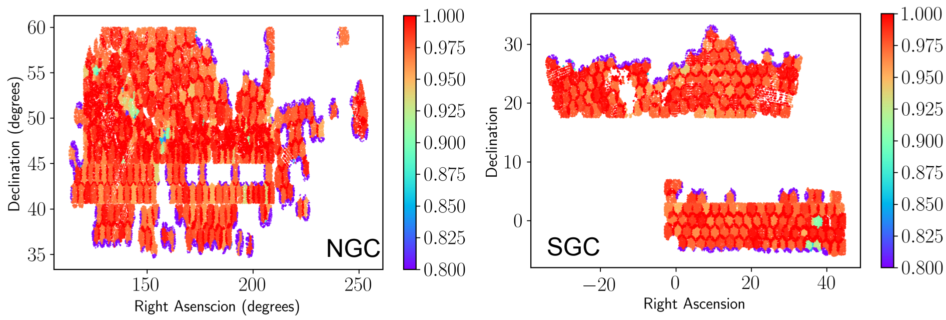

Fig. 1: Footprint of the SDSS-IV DR14 quasar sample color-codded by the completeness that encodes information about various selection effects.

2.1 Redshift uncertainties for eBOSS quasars

Redshift determination proceeds from the analysis of the spectrum of the candidates. Quasar spectra contain broad emission lines due to the rotating gas located around the central super-massive black hole. These features are subject to matter outflows around the accretion disk which frequently give rise to systematic offsets when measuring redshifts.

Figure 2 shows the distributions of $\Delta v = \Delta z \cdot c/(1+z)$, for the difference of redshift estimates: $\Delta z = z_{\rm MgII} - z$, $\Delta z = z_{\rm PCA} - z$ and $\Delta z = z_{\rm PCA} - z_{\rm MgII}$ for the two redshift bins in our range of interest. We compare the discrepancies to a Gaussian distribution of width given by the survey requirements (SRD, Dawson et al. (2016)). The most important feature is that the distributions present large non-Gaussian tails that extend to 3000 km s^{-1}.

The distributions involving $z_{\rm MgII} - z$ (green) and $z_{\rm PCA} - z_{\rm MgII}$ (blue) are centered at zero offset (because of the calibration mentioned above) and are mostly symmetric. The distribution obtained for $z_{\rm PCA} - z$ (red) is asymmetric, suggesting that for the special catalogs which mix $z_{\rm PCA}$ and z, there could be systematic shifts in the separation of quasars. We will demonstrate that the redshift resolution has a large impact on the clustering signal, especially at scales below 40 h^{-1}Mpc, and that the impact can be measured by fitting the data. Furthermore, we will investigate the impact of the redshift resolution on the RSD modeling and on the ability to recover the cosmological parameters both in terms of shape and RMS of the redshift error distribution.

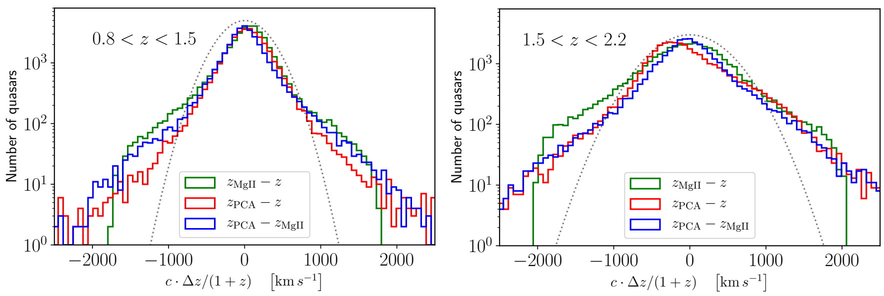

Fig. 2: Physical distributions (solid lines) of $\Delta v = \Delta z \cdot c/(1+z)$ between different redshift estimates for two redshift bins in our redshift range. The dotted line shows a Gaussian distribution of width given by the survey requirements (see text). The most important feature is that the observed distributions present large non-Gaussian tails that extend to 3000 km s^{-1} and that affect the clustering.

3 Full-shape analysis

Contrary to the BAO technique, RSD studies require to model the full-shape of the two-point correlation function (or power spectrum). Measuring the relative clustering in both LOS and perpendicular directions leads to a measurement of the growth rate of structure, but which is degenerate with the AP effect (Alcock & Paczynski 1979). By measuring simultaneously $f\sigma_8$ and the anisotropic positions of the BAO (to derive constraints on $H(z)$ and $D_A(z)$), one can disentangle both effects and provide a measurement of f which does not depend on the fiducial cosmology assumed to convert redshift and angles into distances.

3.1 Modeling of the two-point correlation function in redshift space

The key challenge in modeling RSD is to account for non-linear effects that arise from the non-linear evolution of the density and velocity fields, but also from the non-linear and/or scale-dependent bias between galaxies and matter and the non-linear mapping between real to redshift space. The linear theory formalism is not enough even on scales below $50 - 60\,h^{-1}$.Mpc because of a variety of non-linear effects, including the FOG distortions that occur in collasping and virialized regions at small scales. In order to reach intermediate scales, we adopt a perturbative expansion of the density fields and the bias. In this analysis, we use the Convolution Lagrangian Perturbation Theory (CLPT Carlson et al. (2013); Wang et al. (2014)) with a Gaussian Streaming (GS Reid & White (2011)) model and demonstrate its applicability for dark matter halos of masses of the order of $10^{12.5}$M$_\odot$ hosting eBOSS quasar tracers at mean redshift $z \simeq 1.5$.

3.2 Modeling systematics

We evaluate the performance of the redshift-space modeling using accurate mock catalogs based on an N-body simulation. It allows us to estimate modelling systematics that account for 40% of the statistical precision. In particular, we investigate the two following effects.

Impact of the biasing prescription on dark matter halos The exact number of quasars hosted in satellite halos is not known precisely, and this satellite fraction is degenerate with the duty cycle of quasars that may vary with luminosity and redshift. We test different fractions of satellites in the prescription we apply to dark matter halos to reproduce the observed clustering of eBOSS quasars. Increasing the satellite fraction mildly enhances the amplitude of the clustering, and the quadrupole and hexadecapole are almost unaffected.

Impact of redshift uncertainties The eBOSS quasar sample suffers from an important systematic uncertainty related to spectroscopic redshift precision. Indeed, contrary to galaxies, quasar spectra contain emission lines that can present an intrinsic scatter because of matter outflows around the central super-massive black hole. This systematic uncertainty, which is added to the statistical precision, can therefore affect the estimation of redshift from the fitting of the position of the emission lines. We study the effect of redshift uncertainties by modeling a Gaussian redshift resolution and a more physical resolution using the comparison between different redshift estimates available in the quasar catalog. We demonstrate that accounting for the non-Gaussian tails of the physical distributions has a sizeable impact on the response of the model. In fact, about half of the quoted uncertainty on $\Delta f\sigma_8$ arises from redshift resolution effects.

3.3 Observational systematics

We perform a series of tests to identify and minimize the impact of observational sources of systematic uncertainty in the anisotropic clustering of the eBOSS quasar sample.

Imaging systematics Inhomogeneities in the target selection lead to fluctuations in the target density that affect the clustering. To mitigate this effect, we apply the same *photometric weight* to the data as in Ata et al. (2017) which are based on the 5-σ magnitude detection limit and on Galactic extinction.

Spectroscopic completeness Not all spectroscopic observations provide a valid redshift. We compute a *redshift-failure weight* by tracking the variation of redshift efficiency across the focal plane. This yield a reduction of a factor 3 on $\Delta f\sigma_8$ compared to the standard way where we increase by one unit the weight (upweight) of the nearest neighbour with a good redshift.

Fiber collisions Unmeasured targets due to fiber collision are corrected by upweighting the identified quasar in the collision group (*collision-pair weight*). This approach means that any target within 62" (size of the fiber) of a measured quasar will be displaced along the LOS and brought to the position of the measured quasar. It inevitably creates a lack of objects at all scales and at $\mu \simeq 1$ and hence will affect the correlation function evaluation. In this work, we discard the paircounts in the region close to $\mu = 1$ which is responsible for the remaining systematic shift.

Redshift estimates Different redshift estimates are available in the DR14 quasar catalog to study their impact on the cosmological parameters. We generate different mock realizations of the same redshift uncertainty distribution that are statistically independent and we show that the differences in clustering due to different redshift estimates lie within the expected dispersion and they do not show any systematic trend. We conclude that differences between the results of the fit with the different redshift estimates are due to statistics and we do not quote an additional systematic uncertainty.

We use a set of 1,000 approximate mock catalogs to test the weighting scheme and check to what extent the results on the data are compatible with the mock statistics. These mocks are also used to estimate the covariance of the measurements. Additional tests have been performed on the data, such as using a different covariance matrix or bias prescription. All the tests provide compatible results, suggesting that none of these options affects our estimate of the uncertainty on our cosmological parameters or bias our results by more than 1σ. We therefore only report a modelling systematics for this analysis in configuration space.

4 Cosmological results and conclusions

The full-shape analysis in configuration space and BAO-only analysis have been published in Zarrouk et al. (2018); Ata et al. (2017).

Regarding the Full-Shape analysis, at the effective redshift $z_{\rm eff} = 1.52$, we found $f\sigma_8(z_{\rm eff}) = 0.426 \pm 0.077$ for the growth rate of structure, $H(z_{\rm eff}) = 159^{+12}_{-13}(r_s^{\rm fid}/r_s)$km.s^{-1}.Mpc^{-1} for the expansion rate and $D_A(z_{\rm eff}) =$

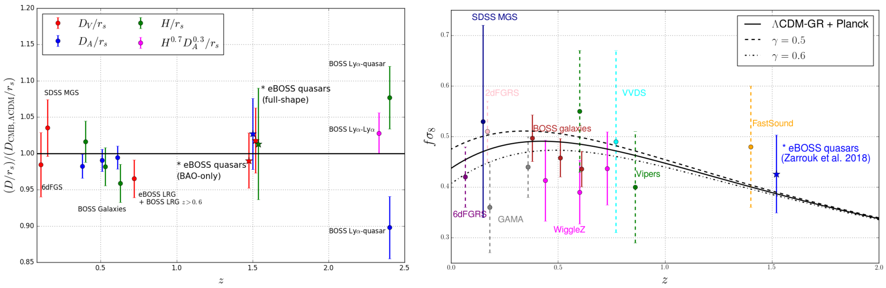

Fig. 3: **Left**: Measurements of BAO distances across redshift. **Right**: Measurements of growth rate of structures across redshift

$1850^{+90}_{-115}\,(r_s/r_s^{\rm fid})$Mpc for the angular diameter distance, where r_s is the sound horizon at the end of the baryon drag epoch and $r_s^{\rm fid}$ is its value in the fiducial cosmology. The quoted uncertainties include both systematic and statistical contributions. The results presented in this proceeding are found to be in agreement with the other companion papers using the same data sample but analysed with different techniques, demonstrating the complementary and the robustness of each method. They are also in agreement with previous measurements from different surveys as shown in Figure 3.

Regarding the BAO-only analysis, it corresponds to the first detection of the BAO in a quasar sample at intermediate redshifts $1 < z < 2$. We obtain a 3.8% measurement on the spherically-averaged BAO distance $D_V(z_{\rm eff} = 1.52) = 3843 \pm 147 (r_d/r_s^{\rm fid})$. Using the BAO data alone from our work and previous independent BAO measurements from BOSS galaxies and Ly-α forests, we tested a ΛCDM model with free curvature, assuming only that the acoustic scale has a fixed comoving size. We find $\Omega_\Lambda > 0$ at 6.6σ significance (Ata et al. 2017).

The results on the evolution of distances from BAO and are consistent with the predictions of ΛCDM with *Planck* parameters assuming the existence of a cosmological constant to explain the late-time acceleration of the expansion of the Universe. The measurement of $f\sigma_8$ is consistent with General Relativity (GR) in the almost unexplored redshift range probed by the eBOSS quasar sample. In this work, we measure simultaneously $f\sigma_8$, D_A and H and obtain a 18% measurement of $f\sigma_8$ after marginalizing over the full set of parameters. When fixing D_A and H, we measure $f\sigma_8$ with 11% precision. Therefore, this work improves the precision of the cosmological parameters, but also extends the inferred cosmological parameters and provides a measurement of the growth rate of structure that can be used to extend the tests of modified gravity models at higher redshift ($z > 1$). We emphasize that measurements of $f\sigma_8$ at fixed D_A and H obtain smaller uncertainties that do not account for the marginalization over the full set of parameters and hence cannot be used to test alternative scenarios of gravity in general. This study is a first use of eBOSS quasars as tracers of the matter field and will be included in the analysis of the final eBOSS sample at the end of 2019 with an expected improvement on the statistical precision of a factor 2. Together with BOSS, eBOSS will pave the way for future programs such as the ground-based Dark Energy Spectroscopic Instrument (DESI) and the space-based mission *Euclid*. Both programs will extensively probe the intermediate redshift range $1 < z < 2$ with millions of spectra, improving the cosmological constraints by an order of magnitude with respect to current measurements.

Pauline Zarrouk thanks warmly the organizers of the session 'Large spectroscopic surveys for cosmology' for the invitation to represent the eBOSS galaxy and quasar clustering working group. Pauline Zarrouk and Etienne Burtin acknowledge support from the P2IO LabEx (reference ANR-10-LABX-0038). Funding for SDSS-III and SDSS-IV has been provided by the Alfred P. Sloan Foundation and Participating Institutions. Additional funding for SDSS-III comes from the National Science Foundation and the U.S. Department of Energy Office of Science. Further information about both projects is available at `www.sdss.org`.

References

Alam, S., Ata, M., Bailey, S., et al. 2017, MNRAS, 470, 2617
Alcock, C. & Paczynski, B. 1979, Nature, 281, 358
Ata, M., Baumgarten, F., Bautista, J., et al. 2017, ArXiv e-prints
Carlson, J., Reid, B., & White, M. 2013, MNRAS, 429, 1674
Dawson, K. S., Kneib, J.-P., Percival, W. J., et al. 2016, AJ, 151, 44
Eisenstein, D. J., Zehavi, I., Hogg, D. W., et al. 2005, ApJ, 633, 560

Guzzo, L., Pierleoni, M., Meneux, B., et al. 2008, Nature, 451, 541
Reid, B. A. & White, M. 2011, MNRAS, 417, 1913
Wang, L., Reid, B., & White, M. 2014, MNRAS, 437, 588
Zarrouk, P., Burtin, E., Gil-Marín, H., et al. 2018, MNRAS, 477, 1639